

# PANCHROMATIC IMAGE PROCESSING USING HYPERSPECTRAL UNMIXING METHOD

Zhenyu An, Zhenwei Shi\*

Image Processing Center,  
School of Astronautics, Beihang University,  
Beijing 100191, P.R. China

Jun Wu, Hongqiang Wang

Remote Sensing and Mapping Department,  
Space Star Technology CO., Ltd.,  
Beijing 100086, P.R. China

## ABSTRACT

In the paper, we consider the probability of applying hyperspectral image (HSI) processing methods to panchromatic images (PIs), which is a novel yet crucial issue for further analyses. To achieve the purpose, we propose an effective approach for handling PI with HSI unmixing methods. In the approach, HSI simulating process is first implemented to obtain a synthetic HSI from PI. After that, a hyperspectral unmixing algorithm, vertex component analysis, is then applied to extract endmembers that comprise the vertices of the data simplex. Meanwhile, we calculate abundances of HSI by employing least squares method. We will see that the unmixing results, namely endmembers and abundances, can be used for target detection and other applications. Different objects such as ships and cars were successfully extracted from the backgrounds, which demonstrates the efficacy of the proposed approach.

*Index Terms*—Panchromatic image processing, hyperspectral image simulating, hyperspectral unmixing, target detection.

## I. INTRODUCTION

**D**IFFERENT representative algorithms such as Vertex Component Analysis (VCA) [1], Constrained Energy Minimization (CEM) [2], and Reed-Xiaoli Detector (RXD) [3] were proposed and successfully applied to the hyperspectral image (HSI) processing by utilizing its substantial spectral information. However, HSI with high spatial resolution is difficult to obtain due to the constraint of spectrometer. Besides, only a small quantity of HSIs are open source data, which brings inconvenience for researchers. On the other hand, panchromatic image (PI), another type of data with only one band, is relatively easier to obtain. With high spatial

resolution (even superior to 1 meter), it contains more spatial information than HSI. However, PI has insufficient spectral information, so most conventional processing methods for PI rely on the development of computer vision and pattern recognition. Features like Histogram of Oriented Gradient (HOG) [4], [5] and Local Binary Patterns (LBP) [6], [8] have been introduced in PI processing and obtain some effective results in target detection and classification.

Spectral resolution, spatial resolution and analyzing methods for HSI and PI have great differences, which lead few researchers to discuss the relationship for the different analyzing methods. No work was reported for PI processing with HSI processing methods to our knowledge. However, in our view, applying the HSI processing methods to analyze PIs is a novel issue, and it is significant for both HSI and PI processing because we could preliminarily establish the relationship between the two different kinds of processing methods. Moreover, it is also practical for the following two reasons. Firstly, both HSI and PI are remote sensing images which share similar data platforms (usually aviation based or space based) and similar ground scenes (usually earth surface). Secondly, conventional HSI processing methods have obtained some effective results although they are originally designed for the HSI, and they also could be applied to images with fewer bands. Therefore, we propose an effective approach for analyzing PI with HSI unmixing algorithms as illustrated in Fig. 1.

Due to the scarce spectral information in PI, we first use the spatial information of PI to synthesize "spectral" information in HSI. Therefore, in the approach, a universal process for HSI simulating is first implemented. HSIs could be obtained with different sampling parameters in the pixel sampling process. After that, hyperspectral unmixing, a significant HSI processing method, is applied to analyze the obtained HSI because of its capability of identifying the constituent materials and estimating the corresponding fractions from the HSI. Unmixing results, especially the obtained abundance maps by using the least squares method (LSM) [11], [12], are useful for the subsequent target detection and other applications. Therefore, the whole approach for handling PI using the HSI unmixing method is established.

The rest of this paper is organized as follows. In Section II,

\*Corresponding author (e-mail: shizhenwei@buaa.edu.cn). The work was supported by the National Natural Science Foundation of China under the Grants 61273245 and 91120301, the Beijing Natural Science Foundation under the Grant 4152031, the Program for New Century Excellent Talents in University of Ministry of Education of China under the Grant NCET-11-0775, the funding project of State Key Laboratory of Virtual Reality Technology and Systems, Beihang University under the Grant VR-2014-ZZ-02, and the Fundamental Research Funds for the Central Universities under the Grant YWF-14-YHXY-028 and the Grant YWF-15-YHXY-003, and the Open Research Fund of The Academy of Satellite Application under grant NO. 2014\_CXJJ-YG\_08.

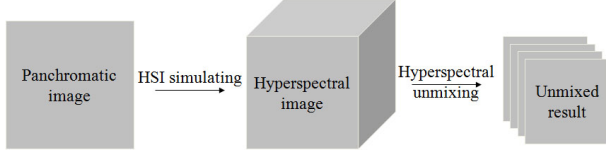


**Fig. 1.** The whole process for PI processing by the hyperspectral methods.

an HSI simulating method is proposed. Based on the linear spectral unmixing model, the unmixing method VCA [1] is briefly introduced and applied to the simulated HSI. In Section III, different experiments are implemented, and we will show the efficacy of the proposed approach. Finally, the paper comes to conclusion in Section IV.

## II. METHODOLOGY

### II-A. HSI simulating

PI, despite its scarce spectral information, has higher spatial resolution than HSI, which prompts us to exploit neighborhood information of its pixels. Therefore, in the simulating process, the neighborhood information will be used to synthesize the spectra of HSI. An example for HSI with 4 bands is illustrated in Fig. 2.

For a given PI  $\mathbf{F}^{L \times K}$ , where  $L$  and  $K$  are respectively the width and height, we use a sliding window to go through it in both horizontal and vertical directions. If the window size  $w \times h$  is  $2 \times 2$  and the sliding step  $s$  is 2, then the total number of pixels in each window is 4. By vectorizing the pixels, we obtain a vector with dimension  $1 \times 4$ . As shown in Fig. 2, the pixels in the left-top and right-down window are vectorized. Then the same managements are implemented on the other pixels and the total number of vectors we obtained for the PI is  $L/2 \times K/2$ . Stacking these vectors together, we obtain an image with 4 "bands" and it has the size  $L/2 \times K/2 \times 4$ . That is the simulated HSI we expect. In the process, two main parameters affect the size of the obtained HSI: one is the sliding window size  $w \times h$ , the other is the sliding step size  $s$ . The band number of HSI relies on the size of sliding window. In our simulating method, the band number is the product of window width and height, namely  $w \times h$ .

### II-B. Hyperspectral unmixing

For an HSI with width and length corresponding to spatial dimensions and the spectral bands as the third dimension (denoted by  $L$ ,  $K$ , and  $S$  in sequence), we vectorize each of its band into a row vector and then obtain the matrix  $\mathbf{V}^{S \times LK}$ . Factorizing the matrix  $\mathbf{V}$  into unmixing results  $\mathbf{W}$  and  $\mathbf{H}$ , the linear spectral mixture model is used which could

be mathematically written as

$$\mathbf{V}^{S \times LK} = \mathbf{W}^{S \times P} \times \mathbf{H}^{P \times LK} + \mathbf{N}^{S \times LK}$$

$$s.t. \quad \mathbf{H}_{ij} \geq 0, \sum_{i=1}^P \mathbf{H}_{ij} = 1 \quad (1)$$

where  $LK = L \times K$ , and  $P$  is the number of endmembers in HSI. Each column of  $\mathbf{W}^{S \times P}$  is an endmember vector which represents a pure object spectrum.  $\mathbf{H}^{P \times LK}$  is the abundance matrix with each row representing the distribution of a corresponding endmember, named abundance map.  $\mathbf{N}$  is the receiver electronic noise. Based on the model, different methods have been proposed for hyperspectral unmixing [9]. VCA [1] is an effective algorithm with the assumption that at least one pure pixel of each endmember is in the data. It could effectively obtain pure pixels and has been widely applied in hyperspectral unmixing. Meanwhile, LSM [12], [13] is used to obtain the abundance map. Target detection will be a natural application by using abundance maps. Different abundance maps represent different specific object distributions, so even a thresholding process on the abundance map could assist us to roughly locate the corresponding targets.

## III. EXPERIMENTS OF APPLICATION TO SHIP AND CAR DETECTION

### III-A. Application in ship detection

Ship detection experiments are implemented on PI as shown in Fig. 3. In the experiments, VCA is applied to obtain the endmember matrix and LSM is applied to calculate abundance matrix. Two groups of parameters for HSI simulating are employed with  $w \times h = 5 \times 5$  and  $w \times h = 8 \times 2$ , respectively. Besides the proposed approach, ship detection methods in [6] and [7] are also implemented and compared with the proposed method. To quantitatively analyze their performances, we derive the receiver operating characteristic (ROC) curves which give the probability of detection (PD) as a function of the probability of false alarm (FPA), as the work in the paper [10]. The unmixing results and ROC curves for different ship detection methods are shown in Fig. 3. Ships are separated from clouds, seas and wharves in Fig. 3(b), which implies that the proposed method with different parameters obtains effective detection results. It is clear that the proposed method with parameters  $w \times h = 8 \times 2$  obtains the best results from the ROC curves in Fig. 3(c), which indicates that the proposed method is a more effective preprocessing step in a complete detection chain.

### III-B. Application in car detection

Besides PI of sea scenes, the proposed method is also applicable to images of other different scenes. As illustrated in Fig. 4, we apply the method to car detection. In the experiment, PI is also obtained from Google map

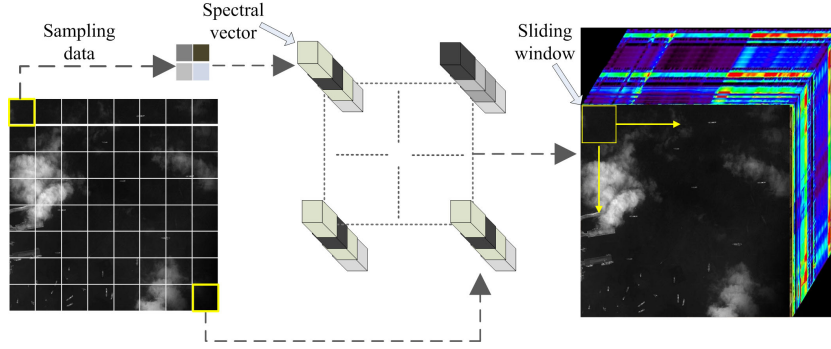


**Fig. 2.** Illustration of HSI simulating process with PI.

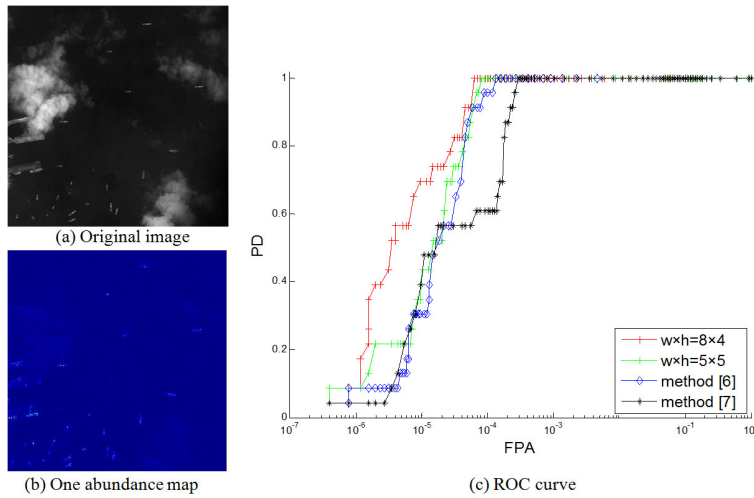


**Fig. 3.** Part of the unmixing result and ROC curves of ship detection results. (a)-(b) Abundance maps with different HSI simulating parameters and endmember numbers.

<https://maps.google.com/> with coordinates of  $39^{\circ}3'32.24''$  N,  $96^{\circ}2'24.75''$  W. The window sizes is  $w \times h = 5 \times 5$ , step sizes is  $s = 1$ , and endmember numbers are set to 8.

Fig. 4(a) is the original PI with size  $567 \times 186$  pixels. Fig. 4(b) and Fig. 4(c) are the corresponding unmixing abundance map and binary map. It is obvious that, by using simple image thresholding, we could effectively separate objects from backgrounds in abundance maps although the contrasts of the original PI is low. Therefore, targets could be precisely located by using other validating processing methods. Overall, the proposed method performs effectively in different object detections, and it could be a critical step in PI processing.

### III-C. Discussion of parameters setting

Three parameters, namely the sampling window size, step size and endmember number, are important to the performance of the proposed algorithm. Some principles are experimentally concluded as follows. Firstly, the window shape should be in accordance with the target shape.

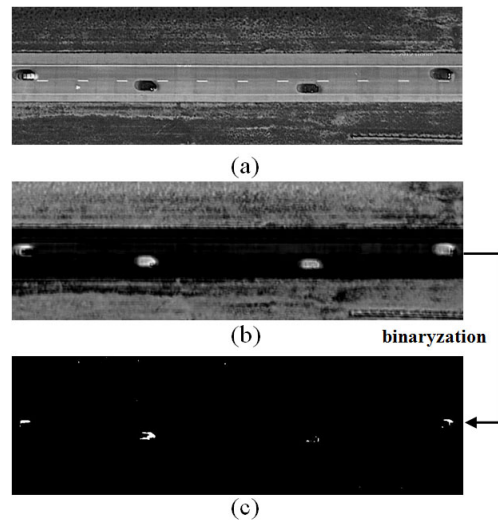


**Fig. 4.** Example for application in car detection. (a) The original image. (b) One abundance map. (c) The abundance map with image thresholding.

Therefore, a window with a rectangle shape obtains a better detection result than the window of square shape in the ship detection experiment. It is better that the window size is set to be smaller than the target size, which makes the spectrum number for the similar object be more in the simulated HSI. Thus in ship and car detections, the window sizes are not larger than those of the targets. For large object like cloud in Fig. 3, the window size is set to  $11 \times 11$ . It is smaller than the cloud size though much larger than the sizes of other objects. Secondly, step size has relatively less influence compared with the window size. It is better that the step size is set to coincide with the object size. The computer memory should also be considered when setting the step size because the smaller step size leads to the larger simulated data size. Thirdly, for endmember number setting, some estimation methods have been proposed although it still remains quite difficult. In our experiment, virtual dimensionality is used to determine the endmember number as proposed in the paper [13].

#### IV. CONCLUSION AND PROSPECTIVE WORK

In the paper, an approach for PI processing with HSI unmixing method is proposed. It provides a novel point of view for analyzing PIs, which encourages us to apply the HSI processing methods to handle PIs. Therefore, the approach establishes an elementary relationship between the methods for PIs and HSIs. The experimental results show that, endmembers of different objects including ships, cars and airplanes, could be successfully extracted from backgrounds like seas and roads by using unmixing method, implying wide potential applications for target detection. From the visual and numerical comparisons, experiment with parameters  $w \times h = 8 \times 2$ ,  $s = 2$  obtains the relatively better results for ship detection in PI, which means that the proposed method exceeds the conventional methods to some extent. It also has to be clear that HSI simulating is the chain between PI and HSI. Besides the proposed sampling window shape used in the paper, methods based on the other specifically designed windows are also available. Meanwhile, more effective unmixing algorithms, even other HSI processing methods, could also be taken into consideration.

#### V. REFERENCES

- [1] J. M. P. Nascimento and J. M. B. Dias, "Vertex component analysis: A fast algorithm to unmix hyperspectral data," *IEEE Trans. Geosci. Remote Sens.*, vol. 43, no. 4, pp. 898-910, Apr. 2005.
- [2] J. C. Harsanyi and C.-I. Chang, "Hyperspectral image classification and dimensionality reduction: an orthogonal subspace projection approach," *IEEE Trans. Geosci. Remote Sens.*, vol. 32, no. 4, pp. 779-785, 1994.
- [3] I. S. Reed and X. Yu, "Adaptive multiple-band cfar detection of an optical pattern with unknown spectral distribution," *IEEE Trans. Acoust. Speech Signal Process.* vol. 38, no. 10, pp. 1760-1770, 1990.
- [4] N. Dalal and B. Triggs, "Histograms of oriented gradients for human detection," *IEEE. Comput. Soc. Conf. on Computer Vision and Pattern Recognition (CVPR)*, pp. 886-893, Jun. 2005.
- [5] M. C. Yeh, K. T. Cheng and S. Avidan, "Fast human detection using a cascade of histograms of oriented gradients," *IEEE. Comput. Soc. Conf. on Computer Vision and Pattern Recognition (CVPR)*, pp. 1491-1498, Jun. 2006.
- [6] Changren Zhu, Hui Zhou, Runsheng Wang and Jun Guo, "A novel hierarchical method of ship detection from spaceborne optical image based on shape and texture features," *IEEE Trans. Geosci. Remote Sens.*, vol. 48, no. 9, pp. 3446-3456, 2010.
- [7] F. Bi, B. Zhu, L. Gao and M. Bian, "A visual search inspired computational model for ship detection in optical satellite images," *IEEE Geosci. Remote Sens. Letters*, vol. 9, no. 4, pp. 749-753, 2012.
- [8] T. Ojala, M. Pietikainen and D. Harwood, "A comparative study of texture measures with classification based on feature distributions," *Pattern Recognition*, vol. 29, pp. 51-59, 1996.
- [9] José M Bioucas-Dias, Antonio Plaza, Nicolas Dobigeon, Mario Parente, Qian Du, Paul Gader, and Jocelyn Chanussot, "Hyperspectral unmixing overview: Geometrical, statistical, and sparse regression-based approaches," *Selected Topics in Applied Earth Observations and Remote Sensing, IEEE Journal of*, vol. 5, no. 2, pp. 354-379, 2012.
- [10] N. Proia and V. Pagé, "Characterization of a bayesian ship detection method in optical satellite images," *IEEE Geosci. Remote Sens. Letters*, vol. 7, no. 2, pp. 226-230, 2010.
- [11] Y. E. Shimabukuro and J. A. Smith, "The least-squares mixing models to generate fraction images derived from remote sensing multispectral Data," *IEEE Trans. Geosci. Remote Sensing* vol. 29, no. 1, pp. 16-20, 1991.
- [12] C.-I. Chang, X. Zhao, M. L. G. Althouse and J.-J. Pan, "Least squares subspace projection approach to mixed pixel classification in hyperspectral images," *IEEE Trans. Geosci. Remote Sensing* vol. 36, no. 3, pp. 898-912, 1998.
- [13] C.-I. Chang and Q. Du, "Estimation of number of spectrally distinct signal sources in hyperspectral imagery," *IEEE Trans. Geosci. Remote Sensing* vol. 42, no. 3, pp. 608-619, 2004.